Elastic Scattering of Alpha Particles by Helium Between 53 and 120 MeV*

P. DARRIULAT,† G. IGO, AND H. G. PUGH
Lawrence Radiation Laboratory, University of California, Berkeley, California

AND

H. D. HOLMGREN‡
University of Maryland, College Park, Maryland

(Received 9 September 1964)

The differential cross section for elastic scattering of α particles by He^4 has been measured at center-of-mass angles between 10 and 90° at laboratory bombarding energies of 53.40±0.15 MeV, 58.49±0.16 MeV, 63.91±0.18 MeV, 69.91±0.20 MeV, 77.55±0.22 MeV, 99.60±0.28 MeV, and 119.86±0.34 MeV. These differential cross sections have been analyzed in terms of complex phase shifts Re $\delta_l + i$ Im δ_l. The real parts of the phase shifts vary smoothly as a function of energy; the $l=0$, 2, and 4 phase shifts continue the trends apparent at lower energies; a broad $l=6$ resonance is found at a center-of-mass energy of about 26 MeV and evidence is found for an $l=8$ resonance. The imaginary parts of the phase shifts are appreciable at all the energies of measurement. The real parts of the phase shifts obtained from these and previous measurements have been fitted with an l-dependent potential constructed from a Saxon-Woods repulsive core and a complex Saxon-Woods attractive well of larger radius. The potential is found to be in qualitative agreement with theoretical predictions. Approximate fits have been made to the real parts of the phase shifts using the single-level dispersion theory. The energies and reduced widths of the resonances given by these fits are approximately proportional to $J(J+1)$.

I. INTRODUCTION

THE interaction between two α particles is of special interest in nuclear physics. Three simplifying features of the interaction make it specially amenable to both experimental and theoretical analysis:

(a) the interacting particles are identical,
(b) both particles have zero spin, and
(c) the particles have a high internal binding energy.

As a result of (a) and (b) the number of phase shifts required to describe the experimental elastic-scattering data is reduced to a minimum, and because of (c) only real phase shifts are required up to a bombarding energy of 35 MeV. In addition, fundamental calculations of the interaction from nucleon-nucleon forces show that the noncentral parts of the forces are unimportant.[1–4] The α-α interaction is of particular importance in nuclear structure theory since the α particle is believed to be an important substructure in more complex nuclei so that a precise knowledge of this interaction may provide a stepping-stone from basic nucleon-nucleon forces to many details of nuclear structure.[5–8]

The elastic scattering of α particles by He^4 has been extensively studied at a number of bombarding energies from 0.150 to 47.1 MeV.[9–11] Good fits have been obtained to the data using the s, d, and g partial waves.[9,12,13] The energy dependence of these phase shifts indicates the presence of resonances at center-of-mass energies of 0.094, 2.9, and 11.7 MeV for the $l=0$, 2, and 4 partial waves, respectively. All three resonances have widths comparable to the Wigner limit. In addition, the general features of the α-α interaction required to fit the behavior of the phase shifts have been elucidated: It is attractive at large distances and becomes repulsive at close quarters, qualitatively very similar to the force between two neutral atoms.

With the Berkeley 88-in. variable-energy cyclotron, high-quality beams of α particles have become available in an energy range hitherto inaccessible. Using it we have measured the elastic-scattering differential cross sections at seven bombarding energies between 53 and 120 MeV. These differential cross sections, analyzed in terms of complex phase shifts, indicate the presence of a broad $l=6$ resonance at a center-of-mass energy of about 26 MeV. In addition, a phenomenological α-α potential has been determined which reproduces the behavior of the phase shifts over the entire energy range from 0.150 to 120 MeV.

* This work was done under the auspices of the U. S. Atomic Energy Commission.
† NATO fellow on leave from Centre d'Études Nucléaires, Saclay, France.
‡ Partly supported by the U. S. Office of Naval Research.
[1] E. Van der Spuy, Nucl. Phys. **11**, 615 (1959).
[2] A. C. Butcher and J. M. McNamee, Proc. Phys. Soc. (London) **74**, 529 (1959).
[3] E. W. Schmid and K. Wildermuth, Nucl. Phys. **26**, 463 (1961).
[4] I. Shimodaya, R. Tamagaki, and H. Tanaka, Progr. Theoret. Phys. (Kyoto) **27**, 793 (1962).
[5] J. A. Wheeler, Phys. Rev. **52**, 1083 (1937).
[6] J. A. Wheeler, Phys. Rev. **52**, 1107 (1937).
[7] K. Wildermuth and Th. Kanellopoulos, Nucl. Phys. **7**, 150 (1958).
[8] K. Wildermuth and Th. Kanellopoulos, Nucl. Phys. **9**, 449 (1958).
[9] T. A. Tombrello and L. S. Senhouse, Phys. Rev. **129**, 2252 (1963) and references therein.
[10] D. J. Bredin, W. E. Burcham, D. Evans, W. M. Gibson, J. S. McKee, *et al.*, Proc. Roy. Soc. (London) **A251**, 143 (1959).
[11] H. E. Conzett, G. Igo, H. C. Shaw, and R. J. Slobodrian, Phys. Rev. **117**, 1075 (1960).
[12] G. Igo, Phys. Rev. **117**, 1079 (1960).
[13] A. T. Berztiss, University of Melbourne (private communication).

II. EXPERIMENTAL ARRANGEMENT AND PROCEDURE

The experimental arrangement and procedure were essentially the same as those described in Ref. 14 where, in particular, a detailed account of the Berkeley 17-in. scattering chamber and tests made to ensure its accuracy is given. Details will be given here only where significant changes from Ref. 14 have been made.

A. Beam Optics

Figure 1 shows the layout of the Berkeley 88-in. cyclotron and the experimental area used in this experiment. The main changes from Ref. 14 are that the beam is now deflected 40° east instead of 20° west and that the quadrupole lens Q2 has been added. Since the beam is deflected in opposite directions in the fringing field of the cyclotron magnet and in the switching magnet, the analyzing powers of the two magnets tend to cancel. To eliminate this cancellation we produce a radial focus between the two magnets by means of the quadrupole lens Q1. Because the radial focusing of the switching magnet is weak, an extra quadrupole lens Q2 is then necessary to help it produce a second radial focus at the fixed position of the analyzing slit AS, which is kept within the cyclotron vault for shielding purposes. After the analyzing slit the beam is focused at the center of the Berkeley 17-in. scattering chamber by means of a third quadrupole lens Q3. At the center of the scattering chamber the beam has the following properties: width, 0.05 in.; height, 0.06 in.; radial divergence, 0.03°; vertical divergence, 0.06°; energy spread, less than 100 keV measured at 65 MeV. The beam intensity used in this experiment was between 0.01 and 0.20 μA (depending on the scattering angle).

B. Beam-Collimation System

We have altered the collimation system before the scattering chamber to improve control over the position and direction of the beam. Three sets of electrically insulated collimators have been installed. The first of these is 28 in. before the center of the chamber, continuously adjustable horizontally and vertically, and water cooled; the second is 8.5 in. before the center; the third is 8.0 in. after the center and is mounted on a mechanism (the internal Faraday cup[14]) which permits it to be removed from the beam when counting is in progress. When the beam is correctly aligned all three of these collimators, just scrape the edges of the beam and opposite sides of each collimator read equal currents. Any unbalance in these currents indicated that the beam direction had changed and could be quickly corrected. With this arrangement the scattering angles in the experiment could be determined to an accuracy of about $\pm 0.01°$.

C. The Gas-Target System

The entire scattering chamber was filled with helium gas at a pressure of about 10 cm/Hg. The entrance window, of 2.5×10^{-5}-in. nickel foil, was directly after the second collimator, and a 10^{-4}-in. Havar foil isolated the helium in the chamber from the Faraday cup vacuum. The energy loss in passing through the system was 250 keV at 100 MeV, of which 50 keV occurred before the target center.

The helium was passed continuously through the chamber, the flow rate being monitored by a flow gauge and the pressure being controlled by a Cartesian manostat which kept the pressure constant to $\pm 0.2\%$. The pressure was read on a Wallace and Tiernan gauge which was calibrated before and after the experiment against an oil manometer and found consistent with the manufacturer's calibration to within 0.1%. The temperature was read on a mercury thermometer attached to the body of the chamber. The pressure, temperature and flow rate were recorded before and after each run and th quantity p/T (proportional to the density) was found to have an rms fluctuation of 0.12%.

D. Counters and Counter Geometry

Three lithium-drifted silicon detectors were used, two mounted on the chamber turrets and one on an arm attached to the target mechanism in the equatorial plane of the chamber. One of the turret counters was

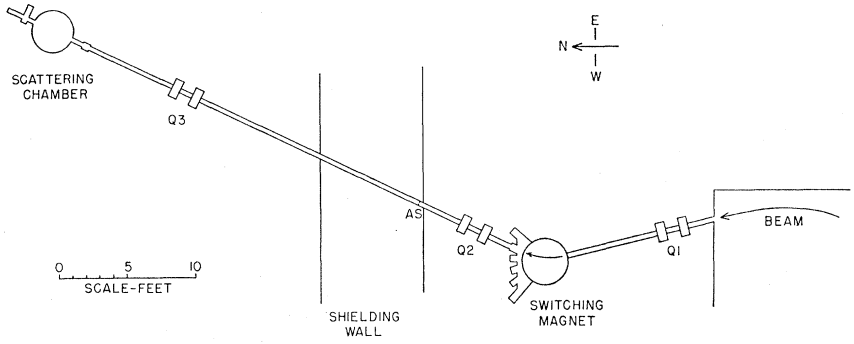

FIG. 1. Schematic layout of cyclotron and experimental area.

[14] P. Darriulat, G. Igo, H. G. Pugh, J. M. Meriwether, and S. Yamabe, Phys. Rev. 134, B42 (1964).

always used as a monitor, fixed on the first maximum in the differential cross section. The equatorial counter permitted the small-angle limit of 10° for the turrets to be overcome. This counter was sufficiently thick to stop 80-MeV α particles and was used mainly at the smaller angles. The two turret counters could stop 70-MeV α particles and were used at larger angles. At 100 and 120 MeV, Al foils placed directly in front of the detectors were used to degrade the energy of the scattered particles when necessary.

Since the counters showed a reduced breakdown voltage when operated in helium at 10 cm Hg, they were isolated from the gas by 10^{-4}-in. Havar windows and operated in air at atomosperic pressure.

The yield at the scattering angle θ contains, for the equatorial counter, the geometrical factor

$$W_1W_2h_2/rd\sin\theta$$

as a first-order approximation, where W_1 is the width of the first counter collimator, W_2 and h_2 are the width and height of the second counter collimator, r is the distance from the chamber center to the second collimator, and d is the distance between the collimators. The values of these quantities are given approximately, in inches, in Table I. For the turret counters θ has to be replaced in this factor by θ_H, the angle between the beam direction and the projection of the scattering angle on the equatorial plane ($\cos\theta=\cos\theta_H\cos 10°$). It is clear that for $\theta_H=0°(\theta=10°)$ the factor is incorrect for the turret counters since the yield will be limited by the height of the first collimator instead of its width. For the collimator sizes used the factor is correct only for $\theta>16°$ assuming a line beam; for a finite beam deviations can occur at angles somewhat larger than this. The turret counters were used mainly at angles greater than 28°, but in a few instances down to 18°, where checks were made for such an effect by comparison with the equatorial counter.

The above first-order geometrical factor has been used in extracting the cross sections. Second-order corrections are less than 0.1%, as are effects due to the finite size of the beam.

The angular resolution is to a very good approximation a triangle of half-width $(W_1+W_2)/2d$ for the equatorial counter (0.55°) and $(W_1+W_2)\sin\theta/2d\sin\theta_H$ for the turret counters (1.19° at 45°, 1.25° at 30°, and 1.54° at 20°).

E. Electronics

The electronics was essentially the same as in Ref. 14, the principal feature being the routing system which ensured that the spectra from all three counters were subjected to the same dead times. These dead times were normally kept down to 1 or 2% by setting the amplifier thresholds to cut out most of the inelastic events and by reducing the beam intensity for the small-angle measurements. To determine the dead times on an absolute basis for correcting the absolute cross section, pulses of fixed amplitude were fed continuously into all the counters during the measurements with a repetition rate modulated by the monitor counting rate.

TABLE I. Gas target geometry: the main dimensions, given in inches. The quantities W_1, W_2, h_2, r, and d are defined in the text.

	W_1	W_2	h_2	r	d
Equatorial counter	0.05	0.05	0.20	8	5
Turret counter	0.125	0.125	0.19	16	6

F. Tests

Measurements was made at small angles on both sides of the beam to check the symmetry about 0°.

Measurements were made at 63.9 MeV up to $\theta_{\text{lab}}=60°(\theta_{\text{c.m.}}=120°)$ and at the other energies up to $\theta_{\text{lab}}=50°$ or 55° to check the symmetry about $\theta_{\text{c.m.}}=90°$.

Measurements were made as a function of gas pressure and of beam intensity to check for turbulence or local heating effects in the gas.

To check that no beam was lost before reaching the Faraday cup as a result of multiple Coulomb scattering the number of counts for a given quantity of collected charge was measured for scattering from a thin nickel foil with and without the windows and gas present.

To check the relative solid angles of the counters a series of overlapping measurements was made.

The results of all the tests were satisfactory within the counting statistics. In particular the excellent agreement obtained for the relative solid angles of the turret and equatorial counters (with different geometry and collimator thicknesses) together with the cleanness of the spectra indicated that slit edge scattering was unimportant.

G. Analysis of the Spectra

The spectra in general presented no analysis problems, the background being negligible.

During some of the measurements small quantities of air were present in the helium, usually less than 0.5%, except for one set of measurements at 58.5 MeV where the contamination was as high as 5.0% for part of the time. At the smallest angles at the lower energies some care was necessary in order to separate the α particles elastically scattered from helium and from air; the uncertainty in this separation has been incorporated into the assigned error. At 58.5 MeV it was, in addition, necessary at some angles to make small corrections for the α particles inelastically scattered from air. The main effect of the contaminant was, however, in altering the density of helium in the chamber since the measured pressure includes the partial pressure of the contaminant. The contaminant was identified as air and its pressure calculated by comparing the elastic scattering angular distributions from the contaminant with the

differential cross-section measurements of Harvey *et al.*[15] on nitrogen and oxygen at 65 MeV and using the scaling law

$$\frac{d\sigma}{d\Omega}(E,\theta_0/E)=(E_0/E)\frac{d\sigma}{d\Omega}(E_0,\theta_0)\,.$$

A small quantity of hydrogen present in the contaminant was consistent with the amount normally present as water vapor in air.

III. RESULTS

A. The Differential Cross Sections

The differential cross sections for the elastic scattering of α particles by He^4 are given in Fig. 2 and are tabulated elsewhere.[16] The uncertainties listed for the individual points include counting statistics and analysis uncertainties. No correction has been made for the finite angular resolution: it is estimated that the effect of this is a few percent in the deepest minima. The uncertainties in the absolute cross sections include geometrical uncertainties, uncertainty in the density of helium due to the presence of contaminants, an allowance for fluctuations of gas pressure and temperature and uncertainty in the calibration of the Faraday cup, and an allowance of about 0.5% for the fact that the rms fluctuation of the monitor counting rate after applying all corrections was somewhat larger than expected. The uncertainty in the energies does not include any possible errors in the range-energy tables used.[17]

The angular distribution at 53.40 MeV is very similar to that at 47.1 MeV,[11] with maxima at 90° and at about 55°. As the energy is increased the angular distributions change systematically: a maximum appears at about 30° and moves slowly to smaller angles while the 55° maximum decreases until barely a trace of it remains at 119.86 MeV. The cross section at large angles decreases rapidly as the energy increases; however, the maximum at 90° persists at all energies though its width decreases slowly with increasing energy.

B. Phase Shift Analysis

The wave function describing a system of two α particles has to be symmetrized with respect to interchange of the two particles. As a result the elastic-scattering differential cross section is described as a function of the center-of-mass scattering angle by the relation

$$\frac{d\sigma}{d\Omega}(\theta)\equiv|f(\theta)+f(\pi-\theta)|^2.$$

The Coulomb amplitude can be extracted in the usual way

$$f(\theta)=f_c(\theta)+f_N(\theta)\,,$$

where

$$f_c(\theta)=(\eta/2k\,\sin^2\tfrac{1}{2}\theta)\,\exp\{-i\eta\ln(\sin^2\tfrac{1}{2}\theta)+2i\sigma_0\},$$

and the nuclear amplitude can be expanded in partial waves

$$f_N(\theta)=\frac{1}{2ik}\sum_l(2l+1)e^{2i\sigma_l}(e^{2i\delta_l}-1)P_l(\cos\theta)\,.$$

In these equations η stands for $4me^2/\hbar k$ where m is the reduced mass of the system, e is the charge of the electron, $\hbar$ is Planck's constant divided by 2π and k is the wave number of the relative particle motion. The Coulomb phase shift σ_l of rank l is defined by the relationship

$$\sigma_l=\arg\Gamma(l+1+i\eta)\,,$$

$P_l(\cos\theta)$ is the ordinary Legendre polynomial of rank l and δ_l is the lth phase shift, which has been made complex to include the effect of inelastic processes: $\delta_l\equiv\mathrm{Re}(\delta_l)+i\mathrm{Im}(\delta_l)$. The imaginary part $\mathrm{Im}(\delta_l)$ must be greater than or equal to zero.

Because of the symmetric form of the wave function, the components of the scattering amplitude with odd l make no contribution while the components with even l are doubled. A similar effect is found in the expansion of the total reaction cross section σ_R which is given by

$$\sigma_R=\frac{4\pi}{k^2}\sum_{l\ \mathrm{even}}(2l+1)(1-|e^{2i\delta_l}|^2)\,.$$

It is straightforward to calculate the angular distributions from the above formulas when the phase shifts are given, but the inverse problem cannot be solved directly. The analysis presented here uses an iterative process to find the phase shifts. An initial set $(\delta_{l,0})$ is chosen, for which the quantity

$$\chi^2=[\alpha_i(\mathrm{exptl})-\alpha_i(\mathrm{theor})]^2\Big/\left\{[\Delta\alpha_i(\mathrm{exptl})]^2+\left[\Delta\theta_i\frac{d\alpha_i}{d\theta_i}(\mathrm{exptl})\right]^2\right\}$$

is calculated, where α_i is written for $d\sigma/d\Omega(\theta_i,E)$, the uncertainty in the measured value of α_i is $\Delta\alpha_i$ and the uncertainty in the angle at which α_i was measured is $\Delta\theta_i$. A new set of values for the δ_l is chosen using the recursion formula

$$\delta_{l,\,r+1}=\delta_{l,r}-D\left(\frac{\partial\chi^2}{\partial\delta_l}\right)_r\Big/\sqrt{\sum_l\left(\frac{\partial\chi^2}{\partial\delta_l}\right)_r^2},$$

where D is a predetermined step length. The procedure is repeated until $\chi_{r+1}^2>\chi_r^2$.

[15] B. G. Harvey, E. J.-M. Rivet, A. Springer, J. R. Meriwether, W. B. Jones, *et al.*, Nucl. Phys. 52, 465 (1964).
[16] P. Darriulat, G. Igo, H. G. Pugh, and H. D. Holmgren, Lawrence Radiation Laboratory Report UCRL-11603, 1964, Table II (unpublished).
[17] C. Williamson and J. P. Boujot, Saclay report, CEA 2189, 1962 (unpublished).

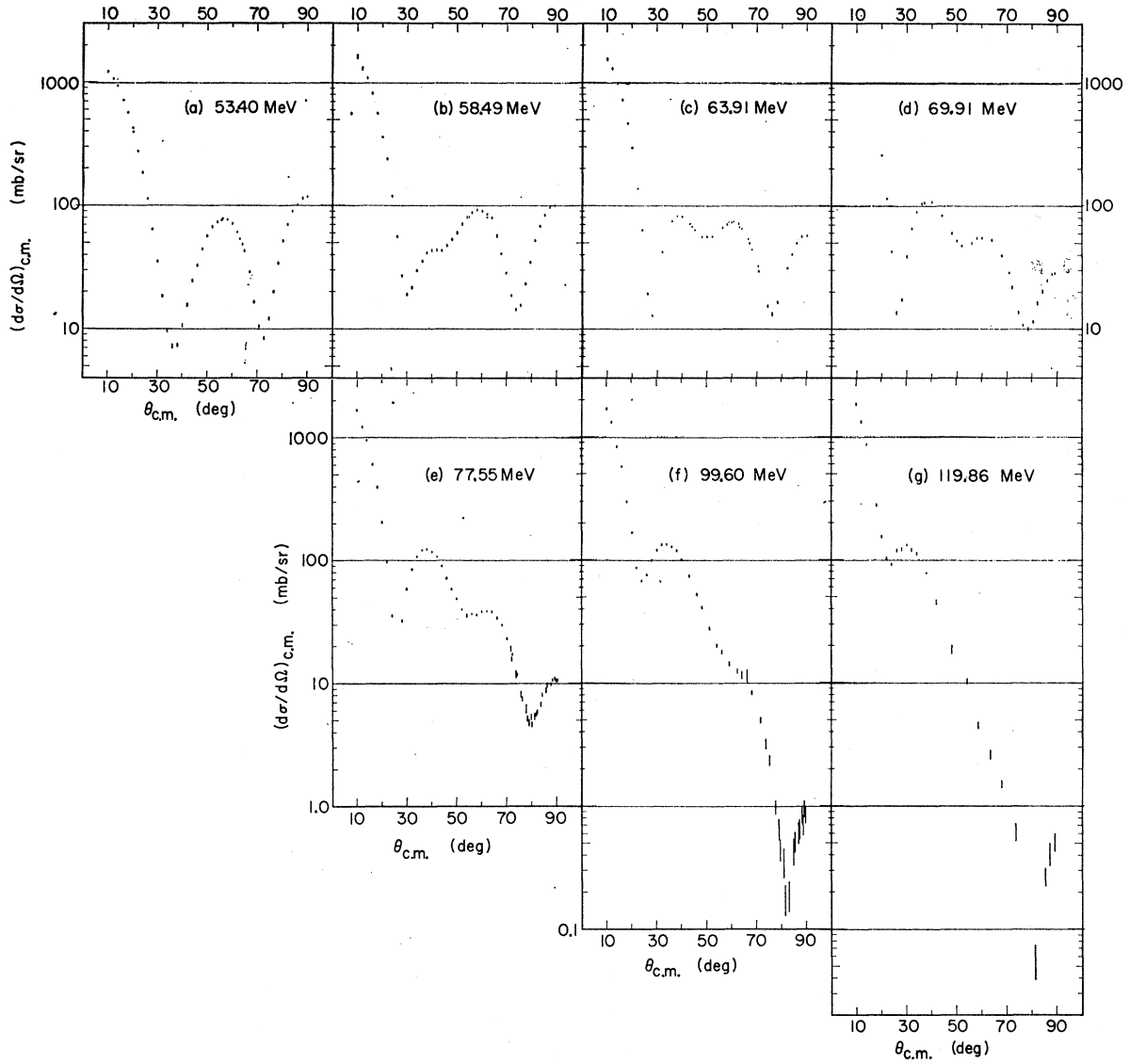

FIG. 2. The differential cross section in the center-of-mass system $(d\sigma/d\Omega)_{c.m.}$ for elastic scattering of alpha particles by helium at laboratory bombarding energies of (a) 53.40±0.15 MeV, (b) 58.49±0.16 MeV, (c) 63.91±0.18 MeV, (d) 69.91±0.20 MeV, (e) 77.55 ±0.22 MeV, (f) 99.60±0.28 MeV, and (g) 119.86±0.34 MeV. The measurements made at center-of-mass angles $\theta_{c.m.}$ greater than 90° are shown at the corresponding angles less than 90°.

The calculation was performed using the Berkeley IBM 7094 computer; one value of the differential cross section was calculated by hand from the phase shifts, checking the machine computation to an accuracy of five significant figures. A step length D of 0.01 rad was used except for final adjustments when it was reduced to 0.001 rad.

As will be shown, partial waves up to $l=8$ or 10 had to be included to fit the data, so that 10 or 12 parameters had to be searched. It was therefore out of the question to use a systematic grid of starting values or to be completely sure that no solution had been missed. We are, however, fairly confident that we have, by the following procedure, found for each energy a set of phase shifts which is either the true one or very close to it.

The differential cross sections were first analyzed in order of increasing energy. At 53.4 MeV the starting set of phase shifts was chosen as that which had fit best the data[11] at 47.1 MeV, the imaginary parts all being taken as zero. For the next energy the fits obtained from the search at 53.4 MeV were used as starting values, and so on for all the energies at which measurements were made. This single series of searches gave for each energy a set of phase shifts with a low value of χ^2. Next, for each energy further searches were conducted using starting phase shifts changed in a fairly random

fashion from those obtained in the first search. At each energy at least one starting set contained all the imaginary parts of the phase shifts set to zero. At the four lowest energies all the searches gave either the same solution as the first one or solutions with completely unacceptable values of χ^2. At the three higher energies several other solutions were found with reasonable low values of χ^2. In these solutions the phase shifts were, however, very close to those for the first set. It is believed that the reason for this result is that the data at the higher energies are less closely spaced in angle and have lower statistical accuracy.

At each energy searches were conducted adding the next higher partial wave. In no case did these give appreciably better fits; the phase shift for this wave was never significantly different from zero and the lower phase shifts were negligibly changed.

The values of χ^2 obtained for the fits are put on a comparable basis by means of the parameter $\epsilon=\chi^2/N$, where N is the number of data points; ϵ should be approximately unity for a perfect fit. The best fits obtained have values of ϵ ranging from 1.0 to 3.4. Since some of these values are statistically improbable it is not possible to use rigorous criteria to specify the uncertainties on the individual phase shifts for these solutions nor to reject solutions with only slightly higher values of ϵ. We have chosen to assign as an error to each phase shift the change that must be made in it (the other phase shifts being kept unchanged) in order to double χ^2. At the energies where several phase shift solutions were found we present those for which ϵ is less than three times that for the best fit.

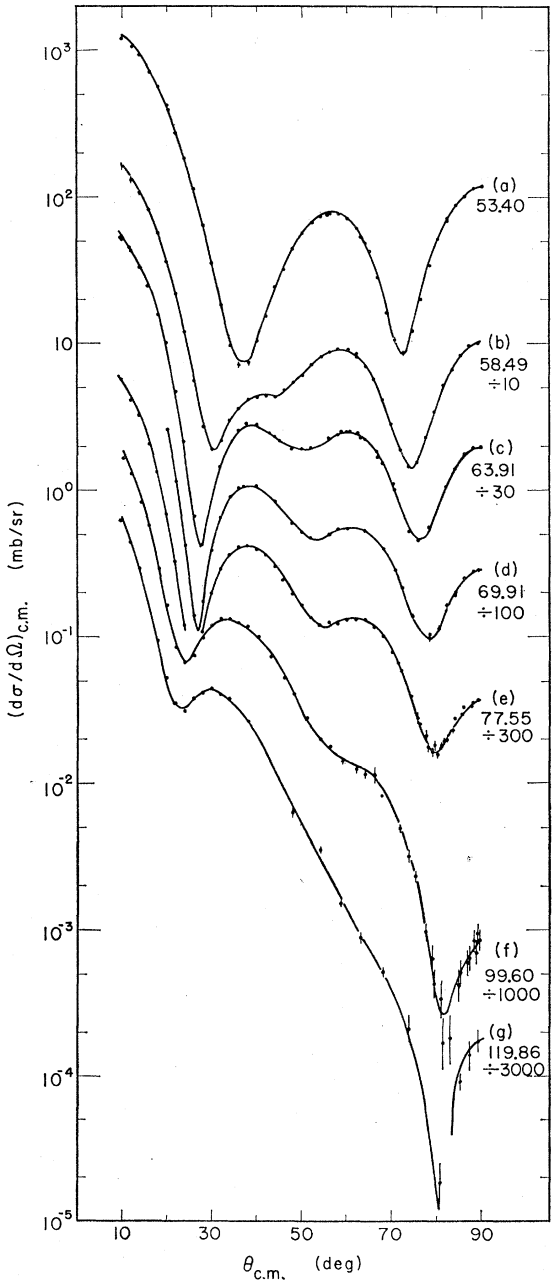

FIG. 3. The fits to the differential cross sections in the center-of-mass system $(d\sigma/d\Omega)_{c.m.}$ given by the phase shifts listed in Table II.

C. The Phase Shifts

The results of the phase-shift analysis are given in Table II together with the total reaction cross sections σ_R calculated from the phase shifts. The fits to the differential cross sections are shown in Fig. 3. The real parts of the phase shifts are plotted in Fig. 4 together with those obtained at lower energies,[9,13] while the imaginary parts of the phase shifts and the calculated total reaction cross sections are shown in Fig. 5.

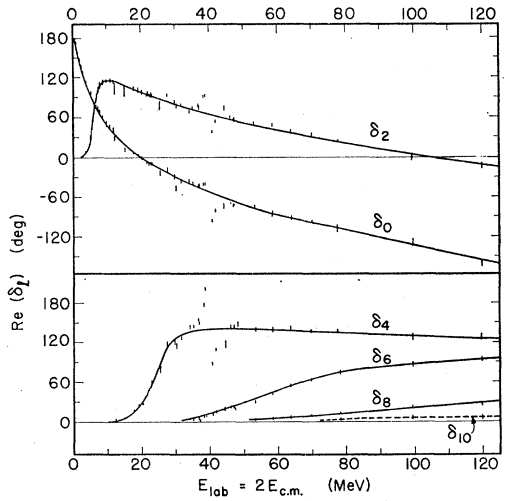

FIG. 4. The real parts of the phase shifts $\mathrm{Re}(\delta_l)$ plotted as a function of the laboratory bombarding energy E_{lab}. The phase shifts below 53.4 MeV were obtained from Ref. 9 and 13. The solid curves are fits given by the potentials listed in Table IV and illustrated in Fig. 6.

TABLE II. The real and imaginary parts of the phase shifts deduced from the analysis presented in Sec. VII. Also listed are the reaction cross sections σ_R in millibarns and the quantity $\epsilon=\chi^2/N$ defined in the text.

Energy (MeV)	ϵ	σ_R(mb)	Re(δ_0)	Re(δ_2)	Re(δ_4)	Re(δ_6)	Re(δ_8)	Re(δ_{10})	Re(δ_{12})
53.40	2.2	649.9	−75.2±2.4	47.9±1.7	137.9±1.3	27.5±0.6	2.0±0.5		
58.49	1.4	687.9	−83.7±2.2	45.6±1.6	138.9±1.5	41.8±0.7	4.0±0.4	0.6±0.4	
63.91	3.4	800.2	−92.5±3.6	38.0±1.8	142.1±1.5	54.2±1.1	6.4±0.5	1.2±0.5	
69.91	1.0	859.3	−97.2±1.8	33.3±1.1	136.1±1.2	63.2±0.8	8.9±0.4	2.4±0.4	
77.55	2.6	848.1	−109.0±4.4	23.4±2.1	136.8±1.9	73.6±2.6	11.7±0.7	2.5±0.7	
77.55	2.7	879.0	−120.9±3.8	16.4±2.1	137.0±1.8	76.6±2.7	9.8±0.7	3.6±0.6	
99.60	1.1	791.5	−129.5±5.7	−2.0±1.7	128.0±1.7	86.7±2.0	21.5±0.7	4.3±0.5	
99.60	1.5	820.7	−140.7±6.4	−4.0±1.9	132.4±1.5	88.9±2.7	17.9±0.9	4.9±0.6	
99.60	1.9	833.3	−126.0±4.3	−6.4±1.9	133.6±1.9	90.0±2.7	16.9±1.2	6.8±0.6	
119.86	1.4	823.9	−161.5±6.3	−16.0±1.7	130.3±1.8	93.8±2.8	26.0±1.4	7.0±0.9	1.7±0.8
Energy (MeV)	ϵ	σ_R(mb)	Im(δ_0)	Im(δ_2)	Im(δ_4)	Im(δ_6)	Im(δ_8)	Im(δ_{10})	Im(δ_{12})
53.40	2.2	649.9	12.1±3.1	22.1±1.7	16.3±1.1	3.2±0.5	0 ±0.4		
58.49	1.4	687.9	10.7±2.3	19.2±1.3	16.4±0.9	6.9±0.6	0 ±0.4	0 ±0.4	
63.91	3.4	800.2	14.2±3.2	18.4±1.9	18.7±1.4	15.8±1.0	0 ±0.6	0 ±0.4	
69.91	1.0	859.3	9.6±2.0	17.9±1.0	20.3±1.0	20.3±0.8	1.9±0.4	0 ±0.2	
77.55	2.6	848.1	18.0±4.6	19.8±2.3	20.1±1.8	27.3±1.5	2.5±0.7	0 ±0.5	
77.55	2.7	879.0	12.2±3.7	18.2±2.1	12.9±1.3	32.8±2.0	4.7±0.8	0 ±0.5	
99.60	1.1	791.5	27.4±6.0	17.0±1.6	20.9±1.6	28.1±1.7	8.5±0.8	0 ±0.5	
99.60	1.5	820.7	26.2±6.9	15.7±1.8	13.2±1.8	27.0±1.8	11.0±1.2	1.0±0.6	
99.60	1.9	833.3	10.8±4.4	13.2±2.0	11.2±1.3	30.3±2.5	15.5±1.4	0.4±0.7	
119.86	1.4	823.9	15.7±3.9	15.6±2.5	13.8±1.6	26.6±1.4	18.3±1.2	3.7±0.6	0 ±0.5

The energy dependence of the real parts of the phase shifts will be discussed in detail in the next section. Here we remark only that they show a remarkably smooth and systematic behavior with the exception of some rapid fluctuations near 40 MeV. These fluctuations are not fully understood and are currently the subject of experimental investigation.[18] Since they occur in a narrow region of energy near the threshold for nuclear reactions and since the phase shifts above and below them can be joined smoothly, we assume that they are not important for an understanding of the general features of the α-α interaction. Similar remarks would apply to any sharp resonance that may occur between two energies of measurement: in this case the correponding phase shift would increase by π in passing through the resonance but outside some narrow energy region would leave no trace on the cross sections.

The imaginary parts of the phase shifts (Fig. 5) show a smooth variation with angular momentum and energy. The $l=0$, 2, and 4 partial waves experience about the same absorption at 53.4 MeV as they do at higher energies. At 53.4 MeV there are already nine reaction channels open, including all the two-body channels. Some of the reaction thresholds (calculated from nuclidic masses given by König *et al.*[19]) are listed in Table III. The $l=6$ and $l=8$ imaginary phase shifts rise with increasing energy in a manner similar to the corresponding real phase shifts, but at slightly higher energies. This shows that most of the reactions occur when the two α particles are still far apart.

[18] H. E. Conzett, E. Shield, R. J. Slobodrian, and S. Yamabe (private communication).

[19] L. A. König, J. H. E. Mattauch, and A. H. Wapstra, Nucl. Phys. 31, 18 (1962).

To see how the absorption affects the differential cross sections, we have calculated these differential cross sections for each energy using the Re(δ_l) from Table II but setting the Im(δ_l) to zero. We find that the effect of the Im(δ_l) is small at small angles but increases rapidly as the angle is increased, while the absorption also smooths out the maxima and minima. Absorption reduces the differential cross section at 90° c.m. by a factor of 2.5 at 53.4 MeV, 9.8 at 99.6 MeV, and 55 at 119.9 MeV.

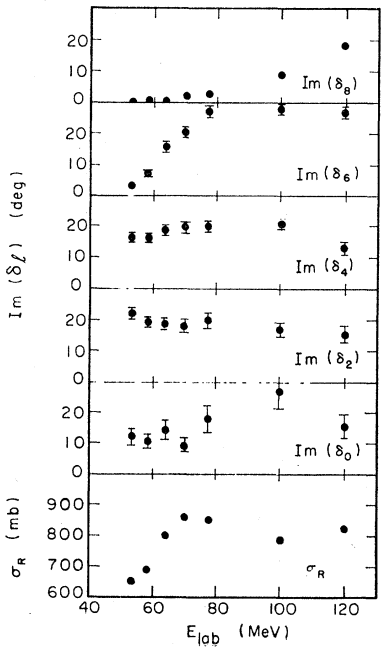

FIG. 5. The imaginary parts of the phase shifts Im(δ_l) and the total reaction cross sections σ_R calculated from them, plotted as a function of the laboratory bombarding energy E_{lab}.

TABLE III. Nuclear reaction thresholds for α-He^4 bombardment, given in the laboratory system. The values are accurate in the last figure quoted and were calculated from nuclidic masses given in Ref. 19.

Reaction fragments	Threshold in laboratory system (MeV)
Li^7+p	34.73
Be^7+n	38.03
He^4+p+t	39.68
He^4+n+He^3	41.21
He^3+He^5	43.1
$t+Li^5$	43.6
Li^6+d	44.82
He^4+2d	44.77
Li^6+n+p	49.28
He^5+p+d	54.2
He^6+2p	54.8
Li^5+n+d	56.2
Be^6+2n	60
He^3+d+t	76.47
$4n+4p$	113.61

The fact that the effects of absorption are already large at 53.4 MeV indicates that the phase shifts obtained at lower energies, but above the threshold for inelastic processes, should be treated with some caution since they were obtained from an analysis using purely real phase shifts. We have attempted not to place any reliance on these phase shifts in the discussion that follows. The only occasion where we have used them is for the $l=6$ partial wave, and our conclusions for this wave are correspondingly weakened. In the analysis of the differential cross sections presented in this paper we did, however, find that the real parts of the phase shifts were rather insensitive to the values used for the imaginary parts, and it is probable that this applies to the lower energy analysis.

IV. INTERPRETATION OF THE PHASE SHIFTS

A. Two-Body α-α Potential

In this section we first recapitulate the arguments which have frequently been made to deduce the approximate form of an effective α-α potential from the energy dependence of the phase shifts at lower energies and expand these arguments to include the new results. We then investigate quantitatively what values for the parameters of such a potential are required to fit the real parts of the phase shifts.

The phase shifts (Fig. 4) all start from zero at zero energy since Be^8 has no bound states. As the energy increases each partial-wave phase shift begins to deviate from zero in the positive direction, at an energy corresponding to an impact parameter of about 5 F, and then passes through resonance. This behavior implies that the nuclear interaction must be attractive at large radii. Above the resonance, the $l=0$ and $l=2$ phase shifts decrease monotonically eventually becoming negative at impact parameters of 1–2 F. This latter behavior indicates that the interaction has a repulsive core of radius 1–2 F. For the higher partial waves the centrifugal barrier prevents investigation of the central regions of the potential; the $l=4$ phase shift has hardly begun to decline at 120 MeV, and the higher phase shifts are still rising. It is informative to note that at 120 MeV the centrifugal barrier is equal to the total energy available in the center of mass system at radii of 1.0, 1.8, 2.7, and 3.7 F for the $l=2$, 4, 6, and 8 partial waves, respectively.

To describe the phase shifts quantitatively we have used a potential of the following form:

$$V(r)\equiv U_1\{1+\exp[(r-r_1)/a_1]\}^{-1} - U_2\{1+\exp[(r-r_2)/a_2]\}^{-1} - iW\{1+\exp[(r-r_3)/a_3]\}^{-1}+V_c(r).$$

The first term represents the repulsive core, the second the larger range attractive potential, the third term allows for inelastic processes, and $V_c(r)$ is the Coulomb potential due to a uniformly charged sphere of radius r_c.

Since the imaginary parts of the phase shifts are not very well determined experimentally we have concentrated in the analysis on the real parts of the phase shifts. These were found to be very insensitive to the following parameters: V_c, W, r_3, a_3, and U_1; we therefore fixed these in the following way:

$$V_c=2\text{ F},$$
$$W=5\text{ MeV},\ E>40\text{ MeV}$$
$$=0,\ E<40\text{ MeV},$$
$$r_3=r_2,$$
$$a_3=a_2,$$
$$U_1\approx 150\text{ MeV}+U_2.$$

With the above choice of values for W, r_3, and a_3, the experimental values of the imaginary parts of the phase shifts were approximately reproduced. Five free parameters remained to be adjusted to fit the real parts of the phase shifts. No automatic search routine was used in adjusting these parameters; the fits to the phase shifts were appreciated by eye.

We first attempted to fit the phase shifts using the same values of the parameters for all the partial waves. This attempt failed: it was found that a more attractive outer region was required for the higher angular momenta. In particular, no set of parameters could be found which would generate $l=4$ phase shifts larger

TABLE IV. The parameters describing the real potentials uses to fit the real phase shifts. The meaning of the uncertainties is defined in the text.

l	U_1 (MeV)	a_1 (F)	r_1 (F)	U_2 (MeV)	a_2 (F)	r_2 (F)
0	150	0.1 ±0.05	1.65 ±0.03	9.2 ±0.5	0.4 ±0.1	3.72 ±0.0
2	150	0.05 ±0.03	1.63 ±0.03	16.0 ±0.2	0.3 ±0.05	3.55 ±0.02
4	220	0.05	1.2	71 ±1	0.46 ±0.03	2.48 ±0.02
6				50 ±2	0.53 ±0.02	2.96 ±0.02
8				110 ±4	0.65 ±0.03	2.00 ±0.05

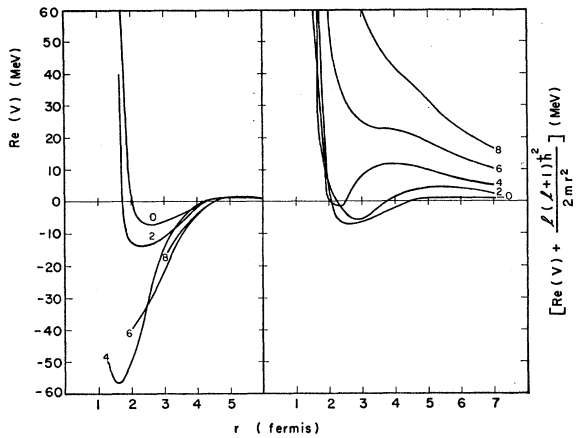

FIG. 6. The real parts of the potentials V used to fit the phase shifts, shown with and without the centrifugal barrier added, plotted against the interaction radius r. The parameters of these potentials are listed in Table IV and the accuracy which they are determined is discussed in the text.

just above the $l=4$ resonance than the $l=2$ phase shifts just above the $l=2$ resonance, as is experimentally observed.

We therefore used a different set of parameters for each partial wave. The best fits obtained in this way are shown in Fig. 3 and the corresponding values of the potential parameters are given in Table IV, where the notation used is that of Nilson *et al.*[20] The uncertainties listed for the potential parameters were obtained by changing the parameters individually; each corresponds to the change that was necessary in an individual parameter to produce a fit judged to be unacceptable. For the $l=4$ wave the values of the parameters for the repulsive core are to be regarded as upper limits, since if the repulsive core is removed the fit to the phase shifts is still acceptable. For the $l=6$ wave the potential has been chosen to fit as well as possible both the phase shifts below 47.1 MeV and those above 53.4 MeV. If the lower energy phase shifts should be altered after reanalysis the $l=6$ potential will be correspondingly altered. If the phase shifts below 47.1 MeV are ignored the attractive part of the $l=6$ potential has a slightly smaller radius.

The values of the parameters given in Table IV are not unique, being subject to a somewhat artificial ambiguity: The Saxon-Woods parametrization we have used has the property that different sets of values of the parameters may give potentials which are very similar outside some value of the range and hence give equally good fits to the data if the scattering does not probe the potential at distances smaller than this value. In the present analysis such ambiguities arose in the definition of the repulsive core for the s and d waves and in the definition of the attractive well for the higher partial waves. Thus for the s and d waves, fits may be obtained by choosing a_1 anywhere between 0 and 0.15 F if r_1 is appropriately adjusted, while the depth parameter U_2 for the $l=6$ and $l=8$ partial waves can be chosen anywhere between 50 and 150 MeV if the smoothness and radius parameters a_2 and r_2 are adjusted to correspond.

The real parts of the potentials are displayed in Fig. 6 as a function of r. Only those parts of each potential corresponding to a total potential (centrifugal+nuclear) smaller than 60 MeV, the maximum energy available in the center-of-mass system for the measurements, are shown. These are the parts of the potentials that are fairly well defined by the experiment.

[20] R. Nilson, W. K. Jentschke, G. R. Briggs, R. O. Kerman, and J. N. Snyder, Phys. Rev. **109**, 850 (1958).

B. Dispersion-Theory Analysis

Other authors have carried out single-level dispersion-theory analyses of the energy dependence of the $l=0$, 2, and 4 phase shifts. In order to compare, in a qualitative sense, the behavior of the $l=6$ and $l=8$ phase shifts with that of the lower ones, we have analyzed them by the same method. Of course one must be careful because of the very broad level widths obtained not to attach too much significance to the results of such an analysis.

We have used for consistency with previous work the notation used in Ref. 20, and since at the higher energies the Coulomb interaction is negligible, have replaced the Coulomb functions $F_l(\rho)$ and $G_l(\rho)$ by $\rho j_l(\rho)$ and $\rho n_l(\rho)$, where j_l and n_l are the regular and irregular Bessel functions of same order.

We found that it is impossible using the single-level dispersion theory to obtain a reasonable fit for either the $l=6$ or the $l=8$ resonance using a single value for the hard-sphere radius. As was previously found for the lower resonances it is possible to obtain a fit only over a small energy range, on the low-energy side of the resonance if a large hard-sphere radius is used or on the high-energy side for a small hard-sphere radius. Table V gives several sets of parameters which fit the phase shifts in various ways; the fits are illustrated in Fig. 7. It will be noted from a comparison of (b) and (c) that even for a given hard-sphere radius there is considerable latitude in the other parameters since different criteria may be used to judge the quality of the fit.

To compare the five resonances so far observed in α-He^4 elastic scattering we have chosen a hard-sphere

TABLE V. Some of the sets of parameters obtained by fitting the i and k resonances with the single-level dispersion relation. The notation used is that of Ref. 20. The fits are illustrated in Fig. 7.

L	a (F)	$\gamma_{\lambda L}^2$ (MeV)	$E_{\lambda L}$ (MeV)	E_{res} (MeV)	$\Gamma_{\lambda L}$ (MeV)	$(2Ma^2/3\hbar^2)\gamma_{\lambda L}^2$
6(a)	3.5	2.3	33.5	36.8	11.4	0.88
6(b)	4.5	2.4	25.3	27.7	16.7	1.52
6(c)	4.5	3.3	26.5	29.5	25.2	2.09
6	5.0	2.0	23.2	24.8	16.6	1.52
8(d)	4.5	6.5	51.2	57	73	4.11

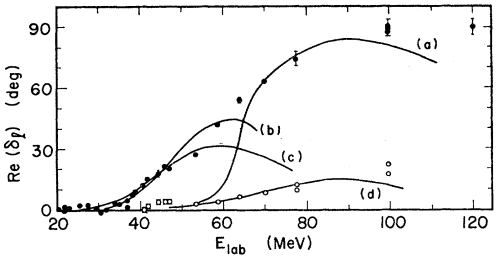

FIG. 7. Single-level dispersion theory fits to the real parts of the $l=6$ and $l=8$ phase shifts, using the parameters listed in Table V, plotted against the laboratory bombarding energy E_{lab}.

radius of 4.5 F for all the resonances, with which value each resonance is fitted well on its low-energy side. This choice, however, has the disadvantage that for the $l=6$ resonance the other parameters are then determined mainly by the phase shifts below 47.1 MeV which, for reasons discussed in Sec. IIIC, may be unreliable, In Fig. 8 we have plotted, for this value of the hard-sphere radius, the energy and reduced width of each resonance against $J(J+1)$. (The parameters for the 0+, 2+, and 4+ resonances are taken from Nilson *et al.*[20] Russell *et al.*[21] and Barker and Treacy.[22]) Both quantities are seen to be almost linear functions of the argument.

V. DISCUSSION

We have shown that the real parts of the phase shifts for α-He^4 scattering at bombarding energies between 53.4 and 119.9 MeV continue the trends which were apparent, apart from fluctuations near 40 MeV, from the low-energy data. The imaginary parts of the phase shifts are appreciable even at 53.4 MeV, suggesting that it might be interesting to re-examine the elastic-scattering data available at energies down to the threshold for nuclear reactions in terms of complex phase shifts, in order to gain further information on the inelastic processes.

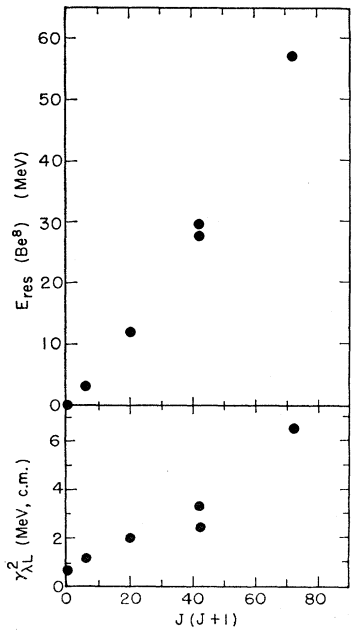

FIG. 8. The excitation energies E_{res} and reduced widths $\gamma_{\lambda L}^2$ for the 0+, 2+, 4+, 6+ and 8+ resonances in Be^8, obtained using a hard sphere radius of 4.5 F, plotted against $J(J+1)$ where J is the spin of the resonance. The two values of E_{res} and $\gamma_{\lambda L}^2$ shown for the 6+ state are for solutions (b) and (c) of Fig. 7 and Table V. The parameters for the 0+, 2+, and 4+ resonances are taken from Refs. 19, 20, and 21.

We have obtained good fits to the real parts of the phase shifts over the energy range from 0.150 to 119.9 MeV with an effective two-body α-α interaction potential in which the parameters are allowed to take on different values for the different partial waves. This potential, like the Margenau[23] and Haefner[24] potentials previously used to analyze α-He^4 scattering, has a repulsive core and an attractive outer region, but its shape is more reasonable in detail. The significant improvement in the shape of the potential lies in the addition of a parameter to allow for smoothness of the outer attractive region; this gave better fits than had previously been obtained to the energy dependence of the phase shifts in the resonance region. The new experimental data at higher energies gave an improved definition of the central regions of the potential and the repulsive core for the $l=0$ and $l=2$ partial waves. An imaginary part was added to the potential for analysis of the higher energy data but the parameters of this absorptive part have not been investigated in detail; we assumed its shape to be the same as that of the attractive part of the real potential.

The use of an l-dependent potential was unambiguously shown to be necessary, as had previously been indicated by the work of Humphrey,[25] Wittern[26] and of Van der Spuy and Pienaar.[27] The extra freedom in fitting given by the l dependence might equally well have been gained by means of a velocity dependence or a nonlocality. The l dependence was chosen for the obvious reason that once the data are represented in terms of phase shifts it is fairly easy to find a potential to fit each partial wave separately.

It is interesting to examine the potentials we have obtained in the light of theoretical predictions. Calculations of the interaction have used the cluster approximation, in which the α particles are assumed to be in their ground state and unpolarized, while the interaction results from the nucleon-nucleon forces which operate between nucleons in the two clusters. Margenau[23] in 1941 rejected this approach firstly because the nucleon-nucleon forces required to provide the outer region of attraction failed to fulfill the saturation requirement, and secondly because the erroneous experimental data available at that time showed a second s-wave resonance at 3 MeV. In the most recent study, that of Shimodaya *et al.*,[4] the saturation argument is

[21] J. L. Russell, Jr., G. C. Phillips, and C. W. Reich, Phys. Rev. **104**, 135 (1956).
[22] F. C. Barker and P. B. Treacy, Nucl. Phys. **38**, 33 (1962).
[23] H. Margenau, Phys. Rev. **59**, 37 (1941).
[24] R. R. Haefner, Rev. Mod. Phys. **23**, 228 (1951).
[25] C. H. Humphrey, Bull. Am. Phys. Soc. **2**, 72 (1957).
[26] H. Wittern, Naturwissenschaften **46**, 443 (1959).
[27] E. Van der Spuy and H. J. Pienaar, Nucl. Phys. **7**, 397 (1958).

rejected since saturation may be obtained as a result of the hard core of the nucleon-nucleon interaction, which does not enter into the α-α interaction. The van der Waals forces resulting from polarization of the α particles, known to be small at low energies,[28] are neglected; only the central nucleon-nucleon forces are retained, and these are obtained from nucleon-nucleon scattering data. Antisymmetrization of the wave function with respect to the nucleon coordinates and spins introduces terms due to one-nucleon and two-nucleon exchange between the clusters and the total potential is the sum of three parts: a static local direct attractive long-range potential and two nonlocal l-dependent potentials arising from the exchange terms. Approximations are then made which are valid at low energies to convert the nonlocal l-dependent potentials into local l-dependent potentials, which have short ranges and are maninly repulsive. The final potential has a strongly repulsive core which becomes weaker for higher l, together with a weakly attractive l-independent outer region.

These results are in qualitative agreement with our findings: The extreme tail of the potential seems to be almost the same for the $l=0$, 2, and 4 partial waves. The $l=6$ and $l=8$ potentials appear to be different in this region; this result should however be regarded with some caution since the $l=6$ potential is mainly determined from the phase shifts between 35 and 47 MeV which for reasons given in Sec. IIIC may be unreliable, while the $l=8$ potential is determined from very sparse experimental information. The repulsive core is less strong for the $l=2$ wave than for the $l=0$ wave, again consistent with the prediction. It would appear that at radii below about 2 F the potential is dominated by the exchange terms and at radii greater than about 4 F by the l-independent direct terms, while between 2 and 4 F the direct and exchange terms are comparable.

It should be remembered that in the theoretical calculations of the interaction various approximations are made which are valid only at low energies, and in particular the possibility of excitation of the α-particle clusters is not included, so that they may not be applicable at the high energies of the present experiment. Taking into account these limitations we find the qualitative agreement between theory and experiment very gratifying.

The single-level dispersion theory fits to the phase shifts are very poor for all the partial waves. This result has been interpreted for the lower partial waves[29] in terms of the potential model as due to the combined effect, felt above resonance, of the repulsive core and the centrifugal potential. The potential analysis given in Sec. IVA shows, however, that the same effect would be observed if the repulsive core did not exist. We prefer to attribute the difficulties in fitting to the extreme smoothness and shallowness of the attractive well.

While it appears that description of the phase shifts by means of a potential is more appropriate than by the dispersion theory, the latter is useful in that it provides a way to correlate some of the properties of the various resonances. The fact that the energies and widths of the resonances are approximately proportional to $J(J+1)$ suggests a rotational description of Be.[8] It should be noted however that the resonance parameters are determined mainly from the low-energy behavior of the phase shifts and do not depend on the interaction at small impact parameters, where the interaction is more strongly l-dependent.

[28] A. Herzenberg and A. S. Roberts, Nucl. Phys. 3, 314 (1957).

[29] C. M. Jones, G. C. Phillips, and P. D. Miller, Phys. Rev. 117, 525 (1960).